Crossed beam reaction of cyano radicals with hydrocarbon molecules. II. Chemical dynamics of 1-cyano-1-methylallene ($CNCH_3CCCH_2$; $X\ ^1A'$) formation from reaction of $CN(X\ ^2\Sigma^+)$ with dimethylacetylene CH_3CCCH_3 ($X\ ^1A_1'$)

N. Balucani,[a] O. Asvany,[b] A. H. H. Chang, S. H. Lin, Y. T. Lee, and R. I. Kaiser[b,c]
Institute of Atomic and Molecular Sciences, 1, Section 4, Roosevelt Road, 107 Taipei, Taiwan, Republic of China

H. F. Bettinger,[d] P. v. R. Schleyer, and H. F. Schaefer III
Center for Computational Quantum Chemistry, Athens, Georgia 30602

(Received 21 June 1999; accepted 28 July 1999)

The reaction dynamics to form the 1-cyano-1-methylallene isomer $CNCH_3CCCH_2$ in its $^1A'$ ground state via the radical–closed shell reaction of the cyano radical $CN(X\ ^2\Sigma^+)$ with dimethylacetylene CH_3CCCH_3 ($X\ ^1A_1'$) are unraveled in a crossed molecular beam experiment at a collision energy of 20.8 kJ mol^{-1} together with state-of-the-art electronic structure and Rice–Ramsperger–Kassel–Marcus (RRKM) calculations. Forward convolution fitting of the laboratory angular distribution together with the time-of-flight spectra verify that the reaction is indirect and proceeds by addition of the CN radical to the π orbital to form a cis/trans $CH_3CNC{=}{=}CCH_3$ radical intermediate. This decomposes via a rather lose exit transition state located only 6–7 kJ mol^{-1} above the products to $CNCH_3CCCH_2$ and atomic hydrogen. The best fit of the center-of-mass angular distribution is forward–backward symmetric and peaks at $\pi/2$ documenting that the fragmenting intermediate holds a lifetime longer than its rotational period. Further, the hydrogen atom leaves almost perpendicular to the C_5H_5N plane resulting in sideways scattering. This finding, together with low frequency bending and wagging modes, strongly support our electronic structure calculations showing a H–C–C angle of about 106.5° in the exit transition state. The experimentally determined reaction exothermicity of 90 ± 20 kJ mol^{-1} is consistent with the theoretical value, 80.4 kJ mol^{-1}. Unfavorable kinematics prevent us from observing the CN versus CH_3 exchange channel, even though our RRKM calculations suggest that this pathway is more important. Since the title reaction is barrierless and exothermic, and the exit transition state is well below the energy of the reactants, this process might be involved in the formation of unsaturated nitriles even in the coldest interstellar environments such as dark, molecular clouds and the saturnian satellite Titan. © *1999 American Institute of Physics.* [S0021-9606(99)01040-5]

I. INTRODUCTION

Investigating the intimate chemical reaction dynamics of the cyano radical $CN(X\ ^2\Sigma^+)$ with unsaturated hydrocarbons is an important means to understand the formation of hydrogen deficient nitriles in various interesting environments such as high temperature combustion flames,[1] hydrocarbon rich planetary atmospheres,[2] and the ultracold ($T=10$ K) regions of the interstellar medium.[3] The outflow of carbon stars with temperatures up to 4000 K close to the photosphere deserve particular attention,[4] since these carbon-rich regions serve as a natural laboratory in which long chain nitriles, among them $H–(C{\equiv}C)_n–CN$ ($n=1–5$) and CCCN can be formed. It often is necessary to set up detailed chemical reaction networks to understand the chemical history of these environments. The most important input parameters for these models are reaction rate constants, the nature of the reaction products, and the branching ratios if multiple exit channels exist. Whereas temperature-dependent rate constants of the reactions of CN with olefins and alkynes have been studied in great detail ranging from very low temperatures down to 15 K,[5] to combustion related scenarios as high as 800 K, the reaction products are often not identified.

Very recently, we initiated a systematic research program aimed to understand the underlying reaction mechanisms of the reactions of CN radical with unsaturated hydrocarbons. We wish to achieve an intimate knowledge of the elementary processes involved as well as the reaction products, i.e., reactions (1)[6] and (2)[7]

$$CN(X\ ^2\Sigma+)+C_2H_2(X\ ^1\Sigma_g^+)\rightarrow HCCCN(X\ ^1\Sigma^+)+H(^2S_{1/2}), \quad (1)$$

[a]Visiting scientist; Permanent address: Dipartimento di Chimica, Università di Perugia, 06123 Perugia, Italy.
[b]Also at: Department of Physics, Technical University Chemnitz-Zwickau, 09107 Chemnitz, Germany.
[c]Author to whom correspondence should be addressed. Electronic mail: kaiser@po.iams.sinica.edu.tw
[d]Author to whom correspondence should be addressed. Electronic mail: bettingr@paul.chem.uga.edu

$$CN(X\,^2\Sigma+)+C_6H_6(X\,^1A_{1g})\rightarrow C_6H_5CN(X\,^1A_1)+H(^2S_{1/2}). \quad (2)$$

To unravel the dynamical information, triply differential cross sections, involved intermediates (if any), and reaction products, we employed the crossed beam technique and conducted the experiments under single collision conditions to avoid a collision-induced stabilization of the intermediate complex(es). This paper elucidates the chemical dynamics of the reaction of cyano radicals with dimethylacetylene CH_3CCCH_3. Our experimental studies are supplemented by electronic structure and Rice–Ramsperger–Kassel–Marcus (RRKM) calculations.

II. EXPERIMENT AND DATA PROCESSING

All experiments are performed under single collision conditions employing the 35′ crossed molecular beam machine.[8,9] Briefly, a pulsed supersonic cyano radical $CN(X\,^2\Sigma^+)$ beam is produced *in situ* via laser ablation of graphite at 266 nm. Molecular nitrogen acts both as a seeding gas and as a reactant with the ablated species. A Spectra Physics GCR 270-30 Nd-YAG laser operates at 30 Hz and 30 mJ per pulse are focused onto a rotating graphite rod. A chopper wheel is located after the skimmer and slices a 9 μs segment of the CN beam with a peak velocity $v_p=1320\pm25\,ms^{-1}$ and speed ratio $S=5.4\pm0.5$. This part of the pulse crosses a second, pulsed dimethylacetylene CH_3CCCH_3, beam ($v_p=790\pm10\,ms^{-1}$, $S=8.4\pm0.4$, 480 Torr backing pressure) at 90° in the interaction region at a collision energy of $20.8\pm0.7\,kJ\,mol^{-1}$ and center-of-mass (CM) angle of $51.2°\pm0.9°$. The reactively scattered products are detected by a triply differentially pumped detector consisting of a Brink-type electron-impact ionizer, quadrupole mass filter, and a Daly ion detector[10] recording time-of-flight spectra (TOF) in 2.5° steps between 7.5° and 72.0° with respect to the CN beam. Data accumulation times range up to 10 h for each angle. Integrating these TOF spectra gives the laboratory angular distribution (LAB). A forward-convolution technique is employed to gain information on the reaction dynamics from the laboratory data.[11] This approach assumes an angular flux $T(\theta)$ and the translational energy $P(E_T)$ trial distributions in the CM coordinate system assuming mutual independence. The final outcome is the generation of a velocity flux contour map $I(\theta,u)$ in the CM frame showing the intensity as a function of angle θ and velocity u. This map contains all the basic information of the scattering process.

III. ELECTRONIC STRUCTURE AND RRKM CALCULATIONS

All our computations performed at the hybrid density functional level of theory using Becke's[12] three-parameter hybrid functional together with the correlation functional of Lee *et al.*[13] as implemented in GAUSSIAN 94.[14] The 6-311 +G** basis set was employed for geometry optimizations and the computation of harmonic vibrational frequencies at stationary points. For all open shell species, the spin unrestricted formalism was employed. All vibrational frequencies and the zero point vibrational energies (ZPVEs) are unscaled. The data reported were obtained at the B3LYP/6-311+G**+ZPVE level of theory.

According to the quasiequilibrium theory or RRKM theory,[15] the rate constant $k(E)$ at a collision energy E for a unimolecular reaction $A^*\rightarrow A^{\#}\rightarrow P$ can be expressed as

$$k(E)=\frac{\sigma}{h}\cdot\frac{W^{\#}(E-E^{\#})}{\rho(E)}, \quad (3)$$

where σ is the symmetry factor and P the product(s). $W^{\#}(E-E^{\#})$ denotes the number of states of the transition state $A^{\#}$ located at the barrier $E^{\#}$. $\rho(E)$ represents the density of states of the energized reactant molecule A^*. The saddle point method was employed to evaluate $\rho(E)$ and $W(E)$ based on our electronic structure calculations. The rate equations corresponding to the reaction mechanism were subsequently solved numerically utilizing the RRKM rate constants. The asymptotic concentrations were adopted as the yields and thus the branching ratios for the products.

IV. RESULTS

A. Reactive scattering signal

First, we investigated the CN versus H exchange channel and observed reactive scattering signal at mass to charge ratio $m/e=79$, i.e., $C_5H_5N^+$. A signal was observed at lower m/e values between 78 and 74 as well, but these TOF spectra show identical patterns to the one at $m/e=79$ and could be fit with the same cm functions. This strongly suggests that the parent species is cracked into the lower masses in the electron impact ionizer. Further, no evidence for a radiative association to give C_5H_6N was found. We attempted to search for the methyl loss channel and checked for $m/e=65$ ($C_4H_3N^+$). However, this channel could not be detected experimentally. Based on the weak reactive scattering signal in the CN versus H exchange, the unfavorable kinematics of the CH_3 loss, and the branching ratios of both channels (as discussed in the following sections), we calculate data accumulation times of at least 50 h at the center-of-mass angle in order to obtain a comparable signal-to-noise ratio as in the H atom loss channel.

B. Laboratory angular distribution (LAB) and TOF spectra

The most probable Newton diagram of the reaction of $CN(X\,^2\Sigma^+)$ with $CH_3CCCH_3(X\,^1A_1')$ to form $CNCH_3CCCH_2(X\,^1A_1)$ and atomic hydrogen $H(^2S_{1/2})$ is shown in Fig. 1 together with the laboratory angular distribution of the product and the best fit. Selected TOF spectra are shown in Fig. 2. The laboratory angular distribution of the heavy C_5H_5N fragment shows a broad peak between 50.0° and 52.5° around the CM angle of 51.2°. This LAB distribution is very narrow and extents only about 30° in the scattering plane. This suggests that the reaction exothermicity is small and/or that the percentage of total available energy channeling into the translation of the products is low. If we compare our observed scattering range with the theoreti-

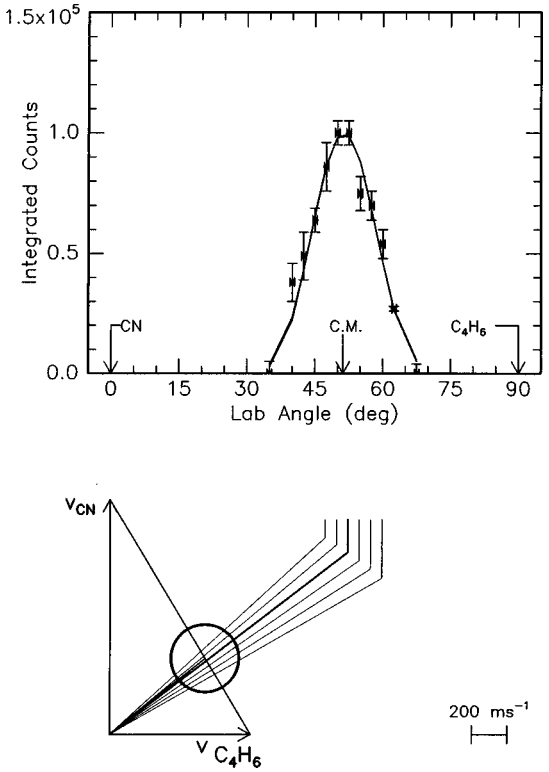

FIG. 1. Lower: Newton diagram for the reaction $CN(X\,^2\Sigma^+) + CH_3CCCH_3(X\,^1A_1') \rightarrow CNCH_3CCCH_3(X\,^1A') + H(^2S_{1/2})$ at a collision energy of 20.8 kJ mol^{-1}. The circle stands for the maximum center-of-mass recoil velocity of the $CNCH_3CCCH_3(X\,^1A')$ product assuming all the available energy is released as translational energy. Upper: Laboratory angular distribution of the $CNCH_3CCCH_3(X\,^1A')$ product. Circles and error bars indicate experimental data, the solid line the calculated distribution.

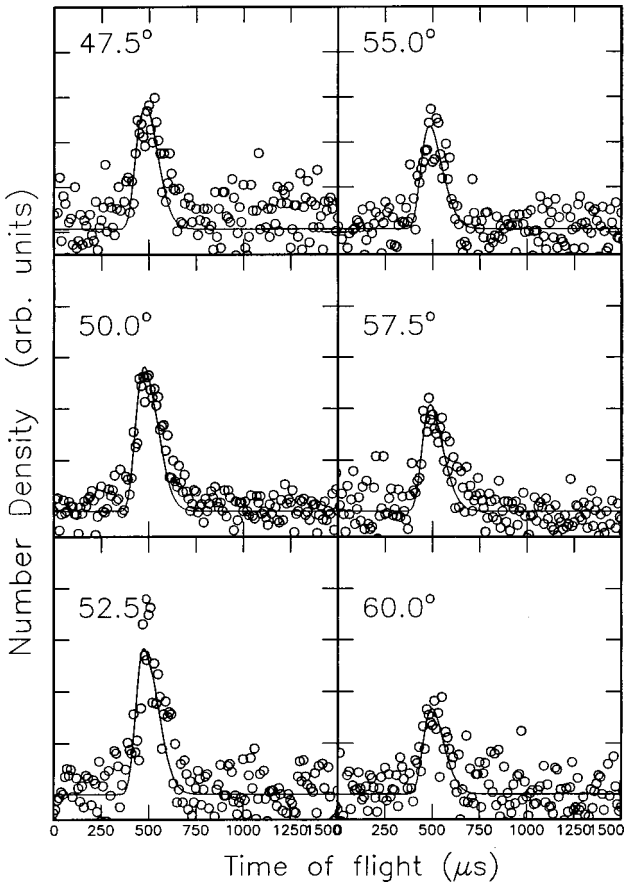

FIG. 2. Time-of-flight data of distinct laboratory angles as indicated in Fig. 1. The dots indicate the experimental data, the solid lines the calculated fit.

cally calculated one and use our *ab initio* exothermicity of 80.4 kJ mol^{-1} to form $CNCH_3CCCH_2$, and construct the Newton circle, we find good agreement with the theory predicting no signal at angles less than 33.0° and larger than 70.0°.

C. Center-of-mass translational energy distribution, $P(E_T)$

Figure 3 depicts the best-fit center-of-mass functions together with those obtained within upper and lower experimental error limits. The best fit translational energy distribution $P(E_T)$ extends to about 110 kJ mol^{-1}. The fits of the laboratory data do not change significantly if we extend or shorten the $P(E_T)$ by about 20 kJ mol^{-1}. Correcting for the collision energy, the title reaction is exothermic by 90 $\pm$20 kJ mol^{-1}. In addition, the $P(E_T)s$ show broad plateaus between 15 and 25 kJ mol^{-1}. This suggests that the exit transition state from the intermediate to the reaction product is likely to be less tight than those in CN reactions (1) and (2) studied previously in our group.[6,7] Therefore, the geometry of the exit transition state is expected to resemble closely the bond distances and angles in the 1-cyano-1-methylallene product. Finally, the experimentally determined fraction of total available energy released into translational energy of the product is 30%–35%.

D. Center-of-mass angular distribution $T(\theta)$ and flux contour map $I(\theta, u)$

The $T(\theta)$ and $I(\theta,u)$ are forward–backward symmetric implying that the reaction follows indirect scattering dynamics via complex formation, cf. Fig. 4. In addition, the symmetry around $\pi/2$ strongly hints that the lifetime of the decomposing complex is longer than its rotational period. A ''symmetric exit transition state'' can be dismissed since no intermediate complex exists in which a rotation can interconvert the leaving hydrogen atom in the decomposing complex (see Sec. V A). The best-fit center-of-mass functions peak at $\pi/2$ with intensity ratios $I(\pi/2)/I(0) = 1.2$. This result strongly indicates geometrical constraints of the direction of the hydrogen atom release in the decomposing intermediate(s) just as found in reactions (1) and (2) (see Sec. V). An isotropic distribution gives a slightly worse fit at the TOF of the center-of-mass angle and the LAB distribution peak.

V. DISCUSSION

A. *Ab initio* C_5H_5N potential energy surface

The highly reactive free cyano radical $CN(X\,^2\Sigma^+)$ attacks the π system of dimethylacetylene without an entrance barrier to give either the *cis* or the *trans* 2-cyano-2-buten-3-yl radicals (**1** and **2**, respectively; *cis* and *trans* refer to the relative position of both methyl groups) in strongly exothermic reactions (see Figs. 5 and 6). Both isomers have C_s

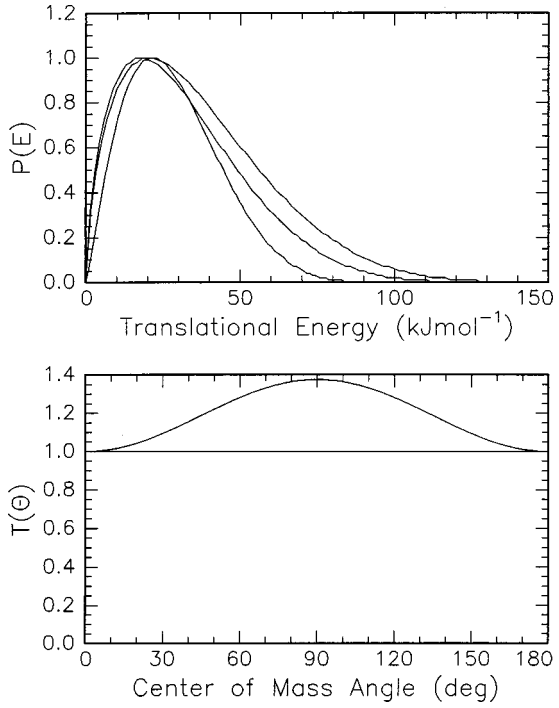

FIG. 3. Center-of-mass angular flux distribution (lower) and translational energy flux distribution (upper) for the reaction $CN(X\,^2\Sigma^+) + CH_3CCCH_3(X\,^1A_1') \rightarrow CNCH_3CCCH_3(X\,^1A') + H(^2S_{1/2})$.

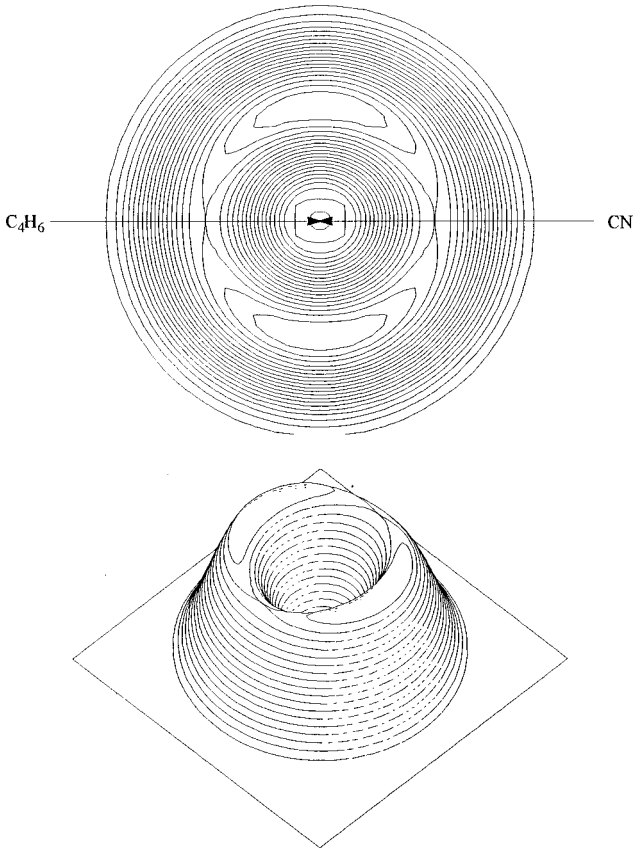

FIG. 4. Center-of-mass velocity contour flux map distribution for the reaction $CN(X\,^2\Sigma^+) + CH_3CCCH_3(X\,^1A_1') \rightarrow CNCH_3CCCH_3(X\,^1A') + H(^2S_{1/2})$. Upper: two dimensional, lower three dimensional plot.

symmetry and a $X\,^2A'$ electronic wave function. Isomer **1** is stabilized by 235.6 kJ mol^{-1} with respect to the reactants. Due to the better alignment of the local dipole moments, the *trans* isomer is slightly more stable by 4.9 kJ mol^{-1} than the *cis* form. The transition state (**TS1**) for isomerization of **1** and **2** is 19.4 kJ mol^{-1} above **1** and hence well below the total energy available in the reaction. The breaking of the in-plane C–H bond of **2** or **1** to give 1-cyano-1-methylallene product and a hydrogen atom is endothermic by 160.1 or 155.2 kJ mol^{-1}. The reaction exothermicity is calculated to be 80.4 kJ mol^{-1}. These reactions involve C_s symmetric transition states (**TS2** and **TS3**) which lie very late along the reaction coordinates. The allene moieties are mostly linear (**TS2**: 177.8 cm^{-1}; **TS3**: 176.5 cm^{-1}, and the 210 pm distances to the departing H atom are much longer than the 110 pm bond lengths in **1** and **2**. In addition, the barriers for the C–H bond cleavage reactions are only slightly (7.5 and 6.7 kJ mol^{-1}) higher than the reaction products.

The cleavage of the C–CH_3 bond to produce 1-cyanopropyne and a methyl radical is an alternative to the C–H bond breaking mechanism. This pathway is more favorable energetically as the overall $CN+CH_3CCCH_3$ reaction energy is larger for alkyne formation (-150.7 kJ mol^{-1}) than for allene formation (-80.4 kJ mol^{-1}). In addition, the exit barrier for CH_3 loss involving C_s symmetric **TS4** is significantly lower (130.9 kJ mol^{-1} with respect to **1**) than the barriers for H loss (155–168 kJ mol^{-1}). The breaking C–C bond is elongated from 152.4 pm in **1** to 229.5 pm in **TS4**, thus indicating the tight character of this transition state. Note that the methyl groups in **TS4** are *cis* as in **1** suggesting that **TS4** connects **1** with **4**. The analogous transition state with *trans* methyl groups could not be located as all such attempts resulted in **TS4**. Hence, the CH_3 loss might not be possible directly from the more stable **2**, where the methyl groups are *trans* oriented, but should first involve the isomerization to **1** via **TS1**.

B. Reaction pathway

The cyano radical, $CN(X\,^2\Sigma^+)$, attacks the π orbital of the dimethylacetylene molecule on the $^2A'$ surface. Since there is no entrance barrier to form the new carbon–carbon σ bond in the *cis* and *trans* $CNCH_3CCCH_3$ collision complexes, the reaction should be dominated by long range induced dipole–permanent dipole and induced dipole–induced dipole interactions. Further, the ultrafast RRKM rate constants of $k_1 = 2.86\times10^{13}\,s^{-1}$ and $k_{-1} = 3.38\times10^{13}\,s^{-1}$ for the isomerizations of both 1-cyano-2-buten-3-yl radicals **1** and **2** (Table II) suggest strongly that the chemical reaction dynamics are independent of the initial concentration of the *cis* versus *trans* intermediates. This is verified by our branching ratios depicting that the CH_3 versus H loss is identical for all initial concentrations of **1** versus **2**. Using the orbiting approximation, we performed an order-of-magnitude calculation of the maximum impact parameter leading to complex formation as well as the maximum accessible rotational quantum number j of **1** and **2**.[16] Based on the value of j and the *ab initio* rotational constants of both intermediates (Table I), we approximate the rotational energy necessary to excite *A*, *B*, or *C* like rotations of the decomposing complex(es).

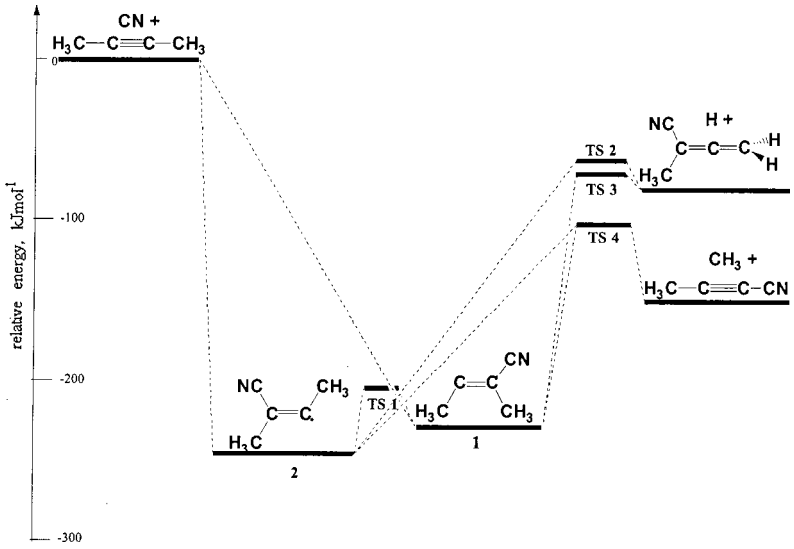

FIG. 5. Schematic representation of the C_5H_6N potential energy surface. Computational details are given in the text.

This procedure shows, that upon complex formation, the heavy atoms of **1** and **2** are rotating most likely in the molecular plane nearly perpendicular to the total angular momentum vector **J** around the *C* axes of the intermediate. Rotations around the *B* and *A* axes are energetically less favored. As observed in our experiments, the doublet radical intermediate(s) have lifetimes longer than their rotation periods of 1.3–1.8 ps and follow a C–H bond rupture through a rather lose transition state to form the 1-cyano-1-methylallene isomer. The experimentally derived exothermicity of $90\pm20\,\mathrm{kJ\,mol^{-1}}$ agrees well with the calculated one of $80.4\,\mathrm{kJ\,mol^{-1}}$. The *j* value as derived within orbiting limits together with energy conservation considerations suggests further that the 1,1-cyanomethylallene product is excited to C like rotations.

The transition states of the H atom loss channel are located only 6–7 $\mathrm{kJ\,mol^{-1}}$ above the products and are less tight than the one in the reaction of cyano radicals with benzene whose exit barrier was derived to be about 32.8 $\mathrm{kJ\,mol^{-1}}$ above the C_6H_5CN and hydrogen atom. This finding correlates with center-of-mass translational energy distributions $P(E_T)$ showing a flux distribution maximum of 15–25 $\mathrm{kJ\,mol^{-1}}$—much closer to zero translational energy than the corresponding benzene reaction. Here, the peak was found between 25 and 38 $\mathrm{kJ\,mol^{-1}}$ documenting that the exit transition state of the latter reaction is tighter than the one of the title reaction. Despite this difference in the exit transition states of both reactions, the geometry of the H atom loss shows a striking similarity in both the CN/CH_3CCCH_3 and CN/C_6H_6 system. Since the best center-of-mass angular flux distribution peaks at 90°, the H atom is emitted parallel to the total angular momentum vector **J** yielding a nearly ''sideways'' peaking of the $T(\theta)$. It is important that the detailed shape of the center-of-mass flux distribution is determined by the disposal of total angular momentum which is given by $\mathbf{J}\approx\mathbf{L}\approx\mathbf{L}'+\mathbf{j}'$.**L** and $\mathbf{L}'$ are the initial and final orbital angular momenta, whereas $\mathbf{j}'$ is the rotational angular momentum of the products. Since the reactants are produced in a supersonic expansion, their rotational angular momentum is expected to be much less than **L**. Herschbach *et al.*[17] demonstrated that if $\mathbf{j}'$ is not zero, $T(\theta)$ is dependent on *J*, *M*, and M'. Here, *M* and M' are the projections of **J** on the initial and final relative velocities, respectively. This model predicts that if a complex decomposes with low M' values, the final velocity $\mathbf{v}'$ is almost perpendicular to **J** and therefore $\mathbf{v}'$ and **v** are almost parallel. Hence $T(\theta)$ is expected to peak at $\theta=0°$ and $\theta=180°$. But when the intermediate dissociates mainly with high M' values, the final relative velocity will be nearly parallel to **J** and perpendicular to **v** and the products will be scattered preferentially at $\theta=90°$. Therefore, our experimental results suggest geometrical constraints of the exit channel, i.e., a preferential emission of the H atom almost parallel to **J**. This is confirmed by our electronic structure calculations: the geometry of the exit transition state is product like, and the hydrogen atom is released at 106.9° and 106.4°, almost perpendicular to the CH_2 unit of the 1-cyano-1-methylallene product (Fig. 6). Together with the low frequency bending and wagging modes the experimentally observed sideways scattering can be observed. The reversed H atom addition has a minimum barrier if the hydrogen atom approaches almost parallel to the π orbital electron density of the $C=CH_2$ moiety. This would allow a maximum orbital overlap between the 1s orbital of the H atom and the π orbital.

We were unable to detect the methyl group elimination channel due to the low signal to noise ratio of the reactive scattering signal and the unfavorable kinematic relationship of the products. However, the calculated branching ratios show that this channel should be dominant. A branching ratio of the CH_3 versus H loss of about 360 is calculated at our collision energy. If we go to 0 $\mathrm{kJ\,mol^{-1}}$ collision energy, i.e., approaching the very cold regions of the interstellar medium, this ratio increases to about 650 (see Table II).

C. Comparison with the reaction $CN(^2\Sigma^+)+CH_3CCH$

The reaction of $CN(^2\Sigma^+)$ with dimethylacetylene has striking similarities to the CN/CH_3CCH system studied earlier in our lab at a comparable collision energy of 24.7 $\mathrm{kJ\,mol^{-1}}$.[18] In both systems, the CN radical attacks a π or-

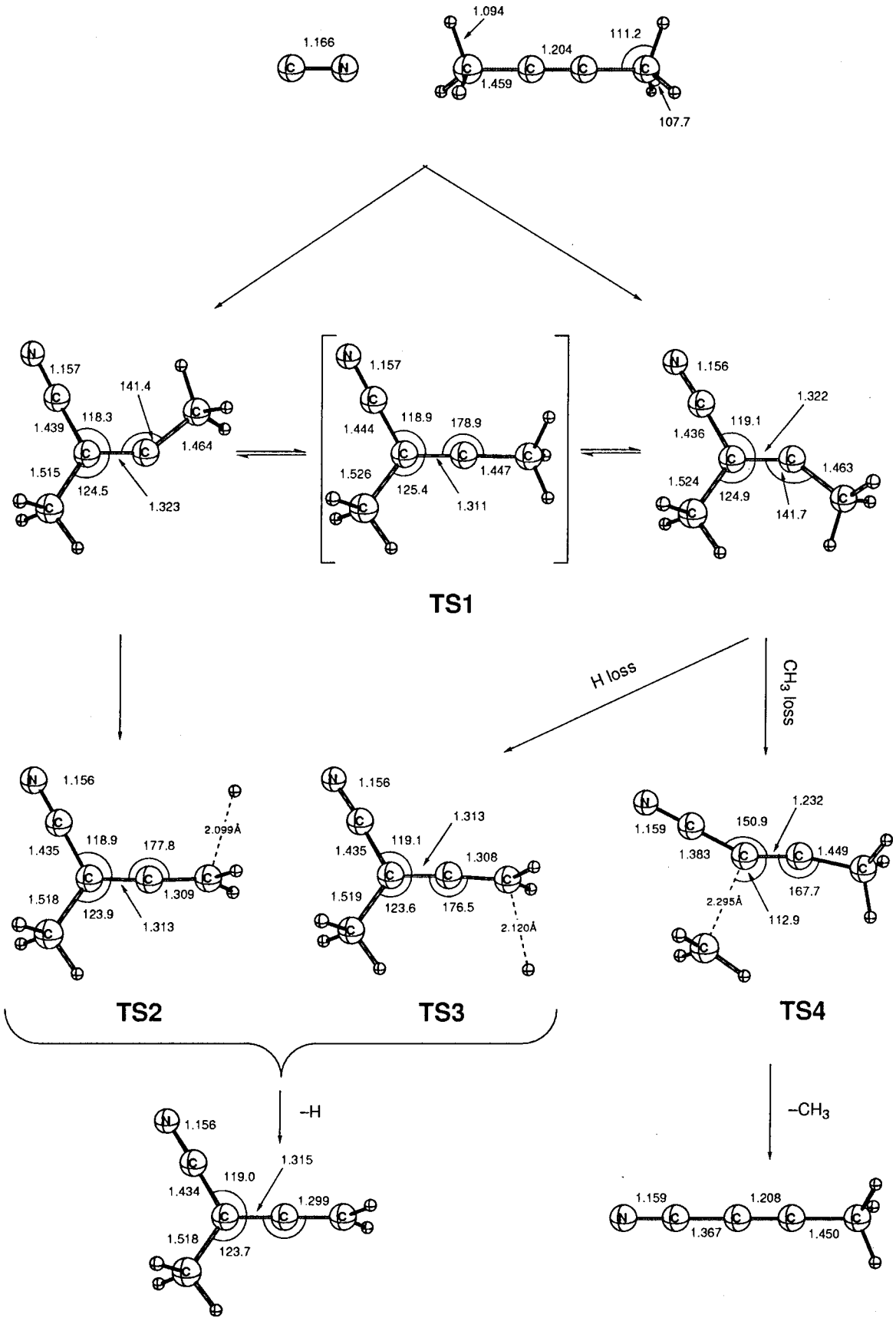

FIG. 6. Bond distances in Angstrom and bond angles in degrees of reactants, intermediates, transition states, and products of the reaction of $CN(X\,^2\Sigma^+)$ with $CH_3CCCH_3(X\,^1A_1')$.

TABLE I. Electronic states, dipole moments μ (D), and rotational constants *A*, *B*, and *C* (GHz) of various molecules at the B3LYP/6-311G** level of theory.

Species	Electronic state	μ	*A*	*B*	*C*
CH_3CCCH_3	$^1A_1'$	0	80.309 123 8	3.363 444 4	3.363 444 4
CN	$^2\Sigma_g$	3.1	0.0	44.762 718 3	44.762 718 3
$CNCH_3CCCH_3$ (*cis*)	$^2A'$	5.4	6.842 649 3	2.290 880 7	1.753 715 6
$CNCH_3CCCH_3$ (*trans*)	$^2A'$	3.8	4.398 551 7	3.183 587 1	1.890 298 1
$CNCH_3CCCH_2$	$^1A_1$	4.4	5.583 067 2	2.705 894 6	1.867 135 5
CH_3CCCN	$^1A_1$	5.4	159.692 261 7	2.076 157 9	2.076 157 9

bital of the alkyne with the carbon atom to form *cis* and *trans* doublet radical complex $CH_3CCCN-X\,(X=CH_3, H)$. Whereas the acetylenic carbon atoms in dimethylacetylene are chemically equivalent, methylacetylene shows two distinct carbon atoms. Here, the sterical and inductive effects of the methyl group are expected to favor an attack at the α C atom, i.e., the one holding the acetylenic H atom. In both cases, the $CH_3CCCN-X$ complexes can fragment via two pathways. The first channel conserves the CH_3 group and forms a substituted methylacetylene; a second pathway involves a C–H bond fission in the CH_3 group giving a substituted allene isomer. This finding suggests that the energy randomization in both systems studied so far is likely to be complete, since the a C–C bond is formed at the α carbon atom, but a C–H bond rupture takes place at the β carbon atom.

VI. CONCLUSIONS

Our crossed molecular beam experiments together with electronic structure and RRKM calculations showed that the reaction of the cyano radical $CN(X\,^2\Sigma^+)$, is governed by indirect scattering dynamics. The reaction proceeds via an initial addition to dimethylacetylene CH_3CCCH_3 without entrance barrier on the $^2A'$ surface to yield two radical intermediates: *cis* and *trans* $CNCH_3CCCH_3$. The *cis–trans* isomerization barrier is well below the total available energy, and the chemical dynamics of the overall reaction are independent of the initial isomer concentrations. The initial addition product rotates around its *C* axis, has a lifetime longer than its rotational period, and fragments via H emission to form 1-cyano-1-methylallene. The experimentally determined reaction exothermicity of 90 ± 20 kJ mol^{-1} agrees well with the theoretical value of 80.4 kJ mol^{-1}. The exit transition states are found to be only $\sim$6–7 kJ mol^{-1} above the products, and are rather loose. Furthermore, the H atom is emitted almost parallel to the total angular momentum vector; this results in a sideways scattering. The explicit identification of the CN versus H atom exchange, the entrance barrierless reaction pathway, and the formation of the 1-cyano-1-methylallene isomer strongly suggests that this reaction might play a role in the formation of unsaturated nitriles in the atmosphere of hydrocarbon rich planets and their satellites such as Saturn and Titan. Although neither the dimethylacetylene reactant nor the final 1-cyano-1-methylallene product have been identified yet, the unsaturated nitriles cyanoacetylene HCCCN, and acyronitrile C_2H_3CN have been observed unambiguously in Titan's stratosphere. Therefore, our results offer a challenging task for the NASA-ESA Cassini–Huygens spacecraft to Titan, which is scheduled to arrive in 2004.[19] Likewise, the methylacetylene molecule has been observed in cold, molecular clouds and old, dying carbon stars in the interstellar medium as well, and dimethylacetylene might also be present as well to form the experimentally observed nitriles in the interstellar medium upon reaction with cyano radicals.

TABLE II. RRKM rate constants in units of s^{-1}.

Collision energy	0 kJ mol^{-1}	20.8 kJ mol^{-1}
k_1[a]	2.58*E*13	2.86*E*13
k_{-1}[b]	3.11*E*13	3.38*E*13
k_2[c]	8.44*E*6	4.77*E*7
k_3[d]	1.25*E*7	6.82*E*7
k_{4t}[e]	6.11*E*9	1.91*E*10
k_{4c}[f]	7.38*E*9	2.26*E*10

[a] k_1 = from 2 to 1.
[b] k_{-1} = from to 1 to 2.
[c] k_2 = from 2 to $CNCH_3CCCH_2+H$.
[d] k_3 = from 1 to $CNCH_3CCCH_2+H$.
[e] k_{4t} = from to $CH_3CCCN+CH_3$.
[f] k_{4c} = from 1 to $CH_3CCCN+CH_3$.

ACKNOWLEDGMENTS

R.I.K. is indebted the Deutsche Forschungsgemeinschaft (DFG) for a *Habilitation* fellowship (Grant No. IIC1-Ka1081/3-1) and Professor D. Gerlich (Technical University Chemnitz, Germany) for support. The work was further supported by Academia Sinica and by the Taiwanese Petrol Organization. The work in Athens was supported by the U.S. Department of Energy, at Erlangen by the DFG and Fond der Chemischen Industrie.

[1] P. R. Westmoreland, A. M. Dean, J. B. Howard, and J. P. Longwell, J. Chem. Phys. **93**, 8171 (1989) and references therein; R. D. Kern, K. Xie, and H. Chen, Combust. Sci. Technol. **85**, 77 (1992).
[2] D. W. Clarke and J. P. Ferris, Origins Life Evol. Biosphere **27**, 225 (1997). F. Raulin *et al.*, ESA Special Publication SP-338 Symposium on Titan 1992, Adv. Space Res. **22**, 353 (1998).
[3] R. I. Kaiser, D. Stranges, Y. T. Lee, and A. G. Suits, Astrophys. J. **477**, 982 (1997).
[4] I. Cherchneff and A. E. Glassgold, Ap. J. **419**, L41 (1993); D. A. Howe and T. J. Millar, Mon. Not. R. Astron. Soc. **244**, 444 (1990).
[5] I. W. M. Smith, I. R. Sims, and B. R. Rowe, Chem.-Eur. J. **3**, 1925 (1997).

[6] L. C. L. Huang, Y. T. Lee, and R. I. Kaiser, J. Chem. Phys. **110**, 7119 (1999).
[7] N. Balucani *et al.*, J. Chem. Phys. **111**, 7457 (1999), preceding paper.
[8] Y. T. Lee, J. D. McDonald, P. R. LeBreton, and D. R. Herschbach, Rev. Sci. Instrum. **40**, 1402 (1969).
[9] R. I. Kaiser *et al.*, J. Chem. Phys. (to be published).
[10] G. O. Brink, Rev. Sci. Instrum. **37**, 857 (1966); N. R. Daly, *ibid.* **31**, 264 (1960).
[11] M. S. Weis, Ph.D. thesis, University of California, Berkeley, 1986.
[12] A. D. Becke, J. Chem. Phys. **98**, 5648 (1993).
[13] C. Lee, W. Yang, and R. G. Parr, Phys. Rev. B **37**, 785 (1988).
[14] M. J. Fritsch *et al.*, GAUSSIAN 94, Revision C.3.
[15] H. Eyring, S. H. Lin, and S. M. Lin, *Basic Chemical Kinetics* (Wiley, New York, 1980).
[16] R. D. Levine and R. B. Bernstein, *Molecular Reaction Dynamics and Chemical Reactivity* (Oxford University Press, Oxford, 1987).
[17] W. B. Miller, S. A. Safron, and D. R. Herschbach, Discuss. Faraday Soc. **44**, 108 (1967); **44**, 291 (1967).
[18] L. C. L. Huang, Y. Osamura, N. Balucani, Y. T. Y. Lee, and R. I. Kaiser, J. Chem. Phys. (to be published).
[19] D. W. Clarke and J. P. Ferris, Icarus **115**, 119 (1995).